Wideband Multi-Resonant Microstrip Patch Antenna for Wireless Communication Systems

Mia Maria Ulfah[1*], Rheyuniarto Sahlendar Asthan[2]

[1]*Department of Telecommunication Engineering, Institut Teknologi Sumatera*
Terusan Ryacudu Road, Way Huwi, Jati Agung, South Lampung 35365, Indonesia

[2]*Department of Electrical Engineering, Institut Teknologi Sumatera*
Terusan Ryacudu Road, Way Huwi, Jati Agung, South Lampung 35365, Indonesia

[*]*Corresponding author. Email: mia.ulfah@tt.itera.ac.id*

Abstract— The increasing demand for high-performance wireless communication systems has driven the development of compact antennas that can support wideband operation, particularly in the 5 GHz frequency range. Microstrip patch antennas (MPAs) remain attractive for such applications due to their low profile and ease of integration, although achieving a wide impedance bandwidth remains a key challenge. This paper presents a low-profile MPA with a wideband response designed for the 5 GHz band of wireless communication systems. The proposed MPA is implemented on a single-layer FR-4 substrate with a thickness of 1.6 mm and is excited using a coaxial probe feed. To achieve a wide impedance bandwidth, a U-shaped patch is utilized as the primary radiator, complemented by a slot, a parasitic element, and a rectangular ring surrounding the main resonator, aiming to generate multiple resonant modes and improve impedance matching. The influence of each modification on antenna performance is systematically analyzed. To validate its performance, the proposed MPA is fabricated and measured, with the obtained results compared to the simulated ones. Simulation and measurement results show good agreement, confirming that the proposed MPA achieves a wideband response with a fractional bandwidth of 18.8% and a peak realized gain of 4.85 dBi. These results highlight the effectiveness of the proposed design and demonstrate its potential for compact and wideband wireless communication devices operating around 5 GHz frequency range.

Keywords— microstrip patch antenna (MPA); multi-resonant modes; parasitic element; U-shaped radiating patch; wireless communication systems

I. INTRODUCTION

High-connectivity wireless networks have become an essential requirement to accommodate the connectivity demands of users in the digital era. These networks encompass various technologies such as Wireless Local Area Networks (WLANs or Wi-Fi) and mobile communication systems. To meet increasing user demands, service providers must deliver systems that ensure high data throughput, seamless connectivity, and robust performance [1]. As these demands continue to rise, wireless technologies have evolved and advanced rapidly to meet modern communication needs. These technologies are not limited to personal use but are also being developed to support various sectors, including industrial, biomedical engineering, and other emerging applications [2], [3].

The reliability of wireless communication technology is primarily determined by its constituent devices, one of which is the antenna, which is integrated to front-end devices to enable the transmission and reception of electromagnetic radiations. In practice, antennas are required to adapt and operate efficiently under dynamically changing propagation conditions. Their performance under those environments is influenced by several factors, including the operating frequency, bandwidth response, and radiation characteristics. For instance, an antenna operating at 5 GHz can provide a higher data transfer rate compared to one operating at 2.4 GHz. However, it exhibits lower penetration capability, and a shorter coverage range due to attenuation and multipath propagation effects at higher frequencies [4], [5]. Furthermore, the antenna bandwidth is essential for supporting high data rates, as it enables greater data transmission capacity [6], [7].

Due to their low-profile and planar structure, microstrip patch antennas (MPAs) have been widely implemented in various applications, including wireless systems. This type of antenna can be realized in various radiating element shapes and is easy to fabricate with a relatively low cost [8]. Another advantage of microstrip antennas is their ease of integration with other microwave devices. However, they generally exhibit a low fractional bandwidth, typically less than 2% [9]. Meanwhile, supporting high data rate communication requires a wider bandwidth to enable more efficient use of the radio frequency spectrum and to accommodate multiple standards within the designated frequency bands.

The impedance bandwidth of an MPA can be improved through several techniques, such as using a thicker substrate, feeding reconfiguration techniques such as proximity coupling, or employing slot or defected ground structure [10] - [12]. Another method is to excite dual or multi-resonant modes. For instance, a concentric shorting pins were utilized to control the even- and odd-order mode positions, thereby achieving an impedance bandwidth of 9% while maintaining a low-profile configuration [13]. In [14], a high-permittivity dielectric feeder was employed to excite a slot-loaded microstrip antenna and generate multiple resonances, resulting in a bandwidth of 45%. However, this configuration leads to a high-profile structure. A

Received 27 October 2025, Revised 25 November 2025, Accepted 26 November 2025.
DOI: https://doi.org/10.15294/jte.v17i2.35545

triple-mode wideband antenna was introduced in [15] by combining two dual-mode antennas with coupled shorted patches and slots. Additionally, in [16], multiple resonances were produced using an anisotropic metasurface and a slot-coupled feed, achieving a bandwidth of 56.1%.

In this work, an MPA incorporating a U-shaped patch, a slot, and parasitic patches is proposed to generate multiple resonant modes. The design employs simple geometric modifications, including the U-shaped patch with a slot and parasitic elements consisting of a rectangular patch and rectangular ring to achieve a wideband response while maintaining a compact, low-profile, lightweight, and simple feeding structure. This design enables multi-resonant wideband performance without relying on thicker substrates or multilayer arrangement. This study presents both design and experimental validation of the proposed wideband MPA intended for 5 GHz wireless communication applications. To demonstrate its performance, the antenna is designed in four different configurations, with the one exhibiting the optimal impedance bandwidth and matching performance subsequently fabricated and measured. The remainder of this paper is organized as follows: the design evolution of the proposed wideband multi-resonant MPA is presented in Section II, the fabrication, measurement setup and its results are discussed in Section III, and conclusions are summarized in Section IV.

II. METHOD

A. Design and Simulation of Multi-Resonant Antenna

The development of the proposed wideband multi-resonant MPA configuration is shown in Figure 1. The antenna is configured on a 1.6 mm thick FR-4 dielectric substrate with a dielectric constant of 4.3. Initially, the configuration of MPA1 incorporates a U-shaped radiating element and is directly excited using a coaxial probe feeding method with an impedance characteristic of 50 Ω as depicted in Figure 1(a). The patch shape, which is utilized to generate dual resonant modes within the desired frequency band, has l_u and w_u of 28 mm and 25 mm, respectively, and an arm width (t_u) of 8 mm. It is important to note that the feed point position significantly influences the excitation of the antenna's resonant modes. In the initial design, the feed point is located at the inner edge of the left arm of the patch. In MPA2, a rectangular slot with a width (s) of 1 mm is introduced into the antenna configuration. This slot symmetrically cuts across the central section of the U-patch, as illustrated in Figure 1(b). Since this slot positioned over the radiating patch can induce a strong electric field around it, its presence could excite or strengthen the antenna's resonant modes within the existing frequency band.

As shown in Figure 1(c), a rectangular parasitic element is employed and arranged at the center of the U-shaped patch, separated by an air gap. This element, which serves as a passive resonator, alters the effective input impedance of the antenna due to mutual coupling with the main radiating patch. This modification aims to improve impedance matching near the antenna's resonant frequency, thereby increasing the fractional bandwidth, while ensuring that the multi-resonant modes do not experience significant shifting. The parasitic patch is configured with l_p and w_p of 19.5 mm and 8 mm, respectively.

The configuration of the proposed MPA as the final design is illustrated in Figure 1(d). It incorporates an additional element in the form of a rectangular ring surrounding the slot-loaded U-shaped patch. The ring has a l_f=32 mm and w_f=28 mm, and t_r =2 mm. The presence of the rectangular ring improves the impedance matching of the first and third resonant

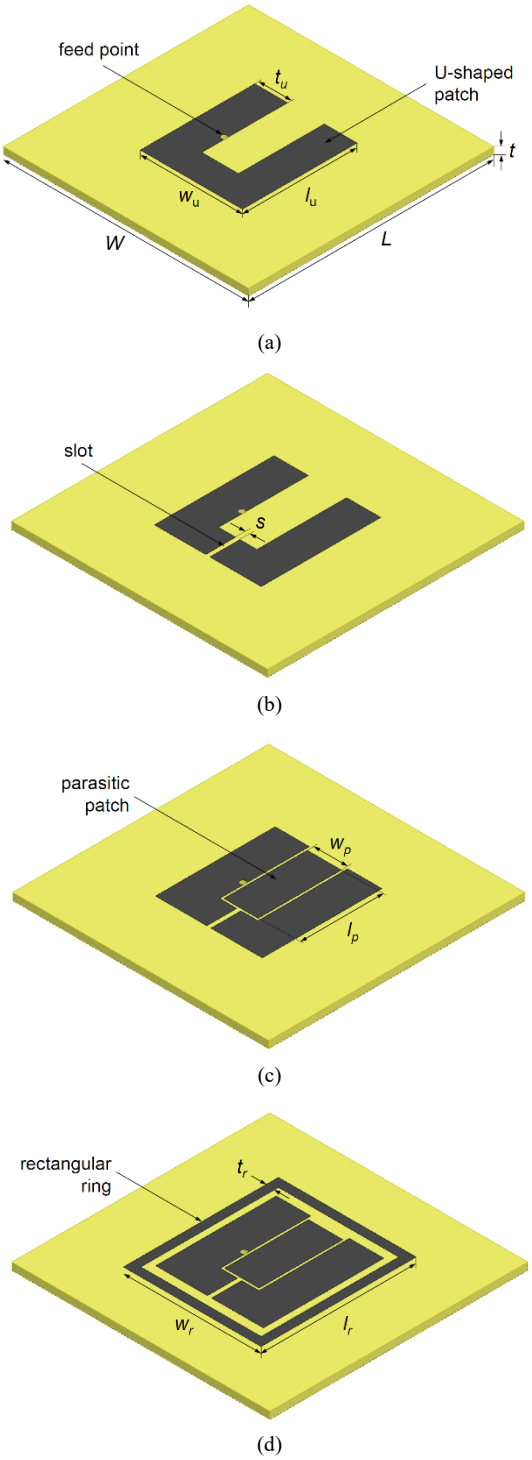

Figure 1. Development of microstrip patch antenna configurations (a) MPA1, (b) MPA 2 (c) MPA 3, and (d) the proposed MPA

frequencies compared to the previous design, while also enhancing the overall operating bandwidth. In addition, variation of the feed point at several locations on the main radiator is also carried out to achieve satisfactory impedance matching over the target frequency band, with the reflection coefficient ($|S_{11}|$) results shown in Figure 2. Notably, the feed locations labelled as point B and E, which share identical x-coordinates but differ in y-coordinates, produce nearly identical results. Among these, point E provides the optimal impedance matching and is therefore chosen as the excitation point for the proposed antenna. The proposed antenna has an overall dimensions L and W of 60 mm × 60 mm, respectively.

To demonstrcoefficientsdwidth improvement among all MPA configurations, the simulated frequency response and

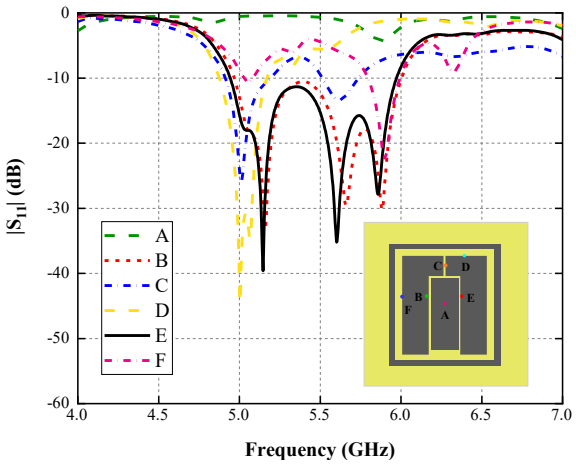

Figure 2. Simulated $|S_{11}|$ of the proposed MPA with various feed location

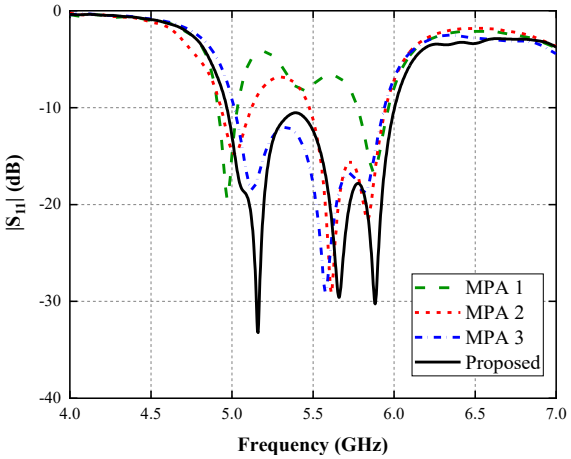

Figure 3. Comparison of the bandwidth performance among different MPA configurations

reflection coefficient are plotted in Figure 3. The results show that MPA1 exhibits two resonant modes, TM_{20} and TM_{21}, at 5.0 GHz and 5.9 GHz, respectively. Meanwhile, the slot-loaded U-shaped patch in MPA2 introduces an additional mode between the first two resonant frequencies, corresponding to TM_{02}, at 5.7 GHz. This configuration produces a multi-resonant response with two adjacent operating bands. The bandwidth is further increased through the incorporation of a parasitic element, achieving a fractional bandwidth (f_{BW}) of 16.8 %. In the final design, the addition of the rectangular ring increases the operating bandwidth from 4.969 GHz to 6.001 GHz, effectively covering the entire 5 GHz band.

Figure 4 shows the current density distribution on the surface of the proposed wideband multi-resonant MPA at three representative frequencies within its operating bandwidth. The simulated results illustrate that the current is highly concentrated on the left arm of the main U-shaped radiating patch, where the radiation intensity is strongest at the lowest mode (TM_{20}), as shown in Figure 4(a), and gradually decreases as the frequency increases. This indicates strong excitation at 5.17 GHz. Furthermore, a noticeable change in the current direction is observed at 5.17 GHz and 5.5 GHz, where the current tends to flow away from the feed point. Meanwhile, at 5.9 GHz, it reverses toward it as a higher-order mode is excited. This change in current distribution confirms the excitation of multiple resonant modes, leading to a wideband antenna response. Moreover, this behaviour could result in distinct radiation characteristics of the antenna at each resonant mode.

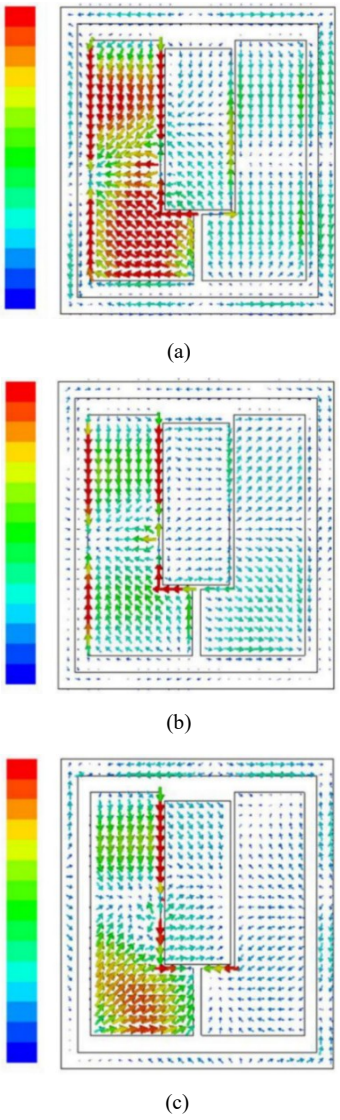

Figure 4. Current density distribution on the surface of the proposed wideband multi-resonant MPA at three different frequencies within the operating bandwidth (a) 5.17 GHz (b) 5.5 GHz, and (c) 5.9 GHz

B. Realization and Measurement of Multi-Resonant Antenna

The proposed wideband multi-resonant MPA was fabricated and experimentally characterized to verify the design and evaluate its actual performance. The prototype of the proposed antenna, which incorporates a slot-loaded U-shaped patch, a parasitic patch, and a rectangular ring, is depicted in Figure 5(a). The antenna was fabricated using an etching process, with FR-4 employed as the dielectric substrate. A 50 Ω SMA connector was used as the excitation probe, with outer and inner conductors soldered to the ground plane and the U-shaped patch, respectively. The dimensions of the fabricated antenna remain consistent with the design at 60 mm × 60 mm × 1.6 mm. The performance of the antenna prototype, referred to as the antenna under test (AUT), was measured and evaluated over the frequency range of 4 GHz to 7 GHz, covering the 5 GHz band. The measurements include the magnitude of $|S_{11}|$, gain and radiation pattern. For the $|S_{11}|$ measurement, the AUT was connected to a vector network analyzer (VNA), while the radiation characteristics were measured inside an anechoic chamber, as illustrated in Figure 5(b). In this setup, the AUT was positioned at a far-field distance from the reference antenna, which in this case is a horn antenna.

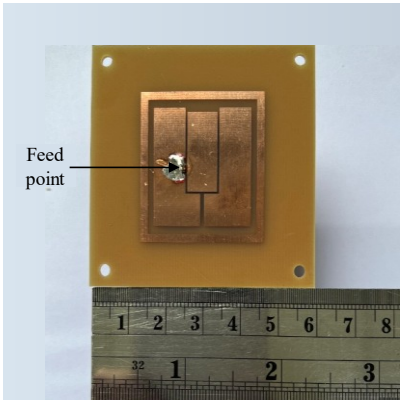

(a)

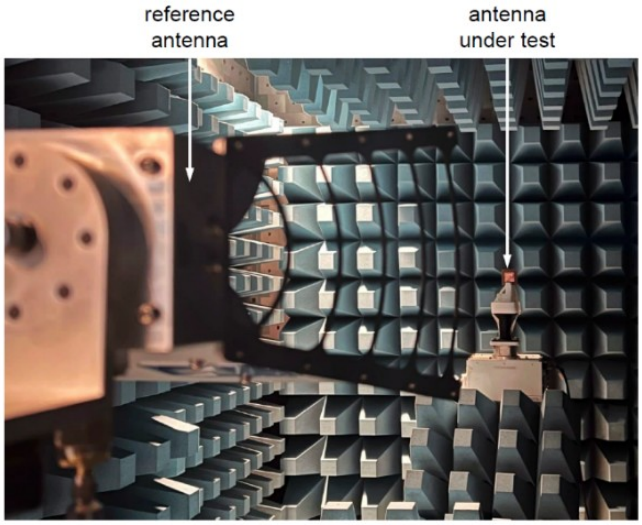

(b)

Figure 5. The proposed antenna (a) Fabricated prototype (b) Experimental setup used for measuring radiation characteristics of the proposed wideband multi-resonant MPA

III. Results and Discussion

Figure 6 compares the simulated and measured $|S_{11}|$ of the proposed MPA. The measured $|S_{11}|$ exhibits a good impedance matching below −10 dB from 4.96 GHz to 5.98 GHz, corresponding to an impedance bandwidth of 18.56%, which agrees well with the simulated result and fully covers the targeted 5 GHz wireless communication band. Additionally, the radiation performance in terms of gain and radiation pattern is plotted in Figures 7 and 8, respectively. From the results, the measured peak gain is obtained at 5.67 GHz with a value of 4.85 dBi, while the simulated one is 5.89 dBi at 5.5 GHz. The slight discrepancy is attributed to fabrication tolerances, soldering issues, and measurement uncertainties.

To further evaluate the antenna performance, Figure 8 compares the simulation and measurement results of radiation patterns at three resonant frequencies, namely 5.17 GHz, 5.5 GHz, and 5.9 GHz, for both co-polarization (red curves) and cross-polarization (blue curves). The co-polarization and cross-polarization components were measured by orienting the AUT along its main polarization and orthogonal axis, respectively, following standard far-field measurement procedure. It can be observed from the measured result that the proposed MPA maintains good polarization in the *E*-plane, showing minimal unwanted orthogonal radiation across the operating bandwidth. This is indicated by the strong cross-polarization suppression, particularly at the lower frequencies of 5.17 GHz and 5.5 GHz. However, at 5.9 GHz, a slight increase in the cross-polarization

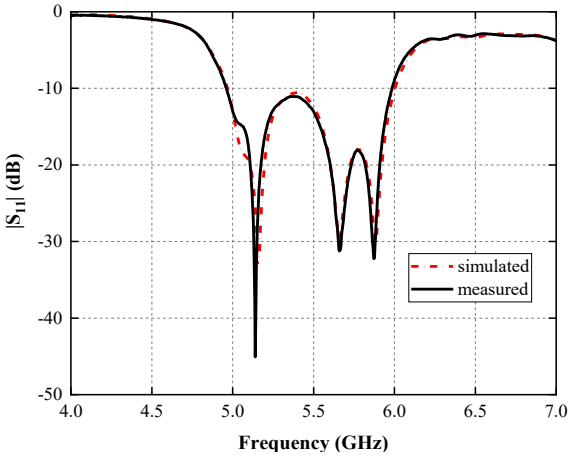

Figure 6. Simulated and measured $|S_{11}|$ of the proposed wideband multi-resonant MPA

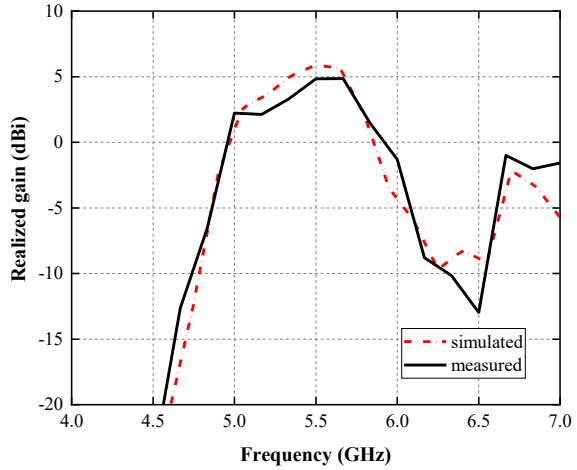

Figure 7. Simulated and measured realized gain of the proposed wideband multi-resonant MPA

TABLE I. Performance Comparison with Related Works.

Ref.	Antenna Type	f_0 (GHz)	f_{BW} (%)	Peak gain (dBi)	Profile (λ_0‡)
[17]	MPA	5.80	8.5	10.5	0.030
[18]	HMSIC	5.50	15.7	7.1	0.058
[19]	HMA	5.45	18.1	10.9	0.068
[20]	DPR	5.00	20.3	7.7	0.061
[21]	MPA	5.50	16.5	10.4	0.073
[22]	DRA	5.15	26.0	8.2	0.190
This work	**MPA**	**5.50**	**18.5**	**4.8**	**0.035**

‡λ_0: the free-space wavelength corresponding to the center frequency (f_0) of the antenna.

level is seen due to mutual coupling between the main radiating patch and the rectangular ring. A similar behavior is observed in the *H*-plane, where the effect becomes more pronounced at higher frequencies. This effect is also reflected in the gain performance, where a lower gain is achieved at 5.9 GHz. Moreover, although the main beam is slightly tilted from the normal direction due to asymmetric excitation in both planes, the measured radiation patterns closely agree with the simulated ones.

Table I presents the performance comparison between the proposed wideband multi-resonant MPA and other reported wideband antennas operating in the 5 GHz frequency band [17-22]. The antenna reported in [17] achieved a high gain of 10.5 dBi and an impedance bandwidth of 8.5%, which was obtained by exciting a higher-order mode through careful tuning of the meander line dimensions. In contrast, a high gain half-mode substrate integrated cavity (HMSIC) was proposed for WLAN applications, offering a 15.7% bandwidth through the

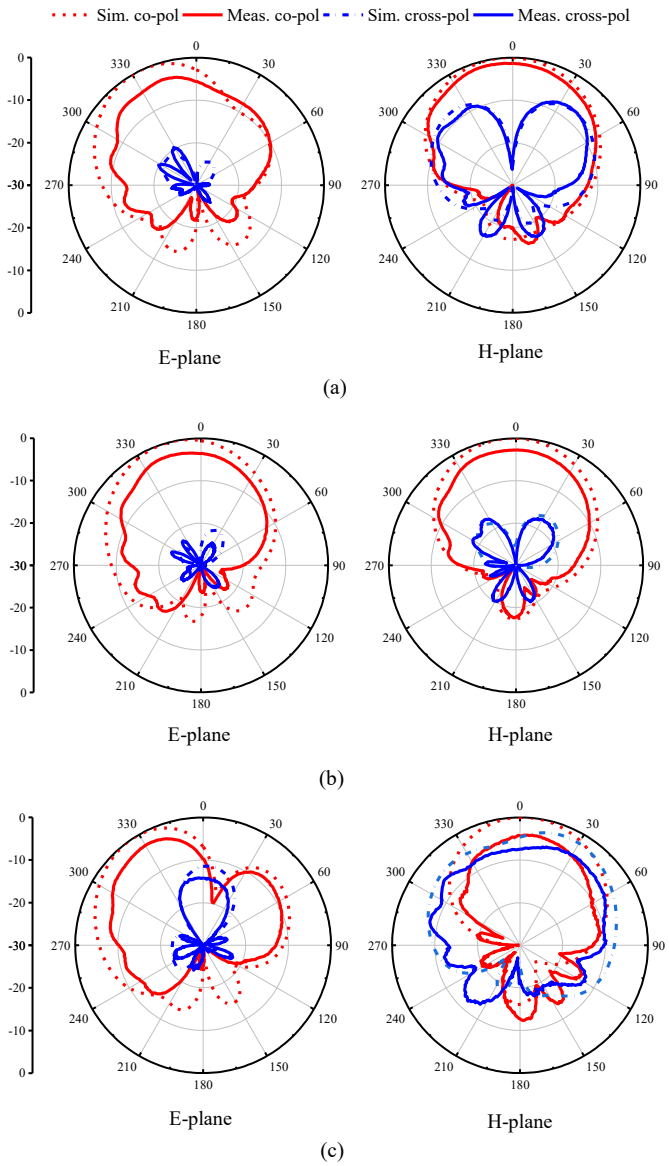

Figure 8. Simulated and measured radiation patterns of the proposed wideband multi-resonant MPA at three frequencies within the operating bandwidth (a) 5.17 GHz (b) 5.5 GHz, and (c) 5.9 GHz

incorporation and optimization of a slot structure [18]. Compared with the proposed wideband multi-resonant MPA, which maintains a comparable profile, the design in [17] provides a narrower impedance bandwidth, limiting its use in wideband scenarios. Similarly, the HMSIC in [18] exhibits a slightly smaller bandwidth and a relatively higher overall profile due to the use of a thicker substrate.

Furthermore, compared with other reported designs, the proposed antenna achieves a balanced trade-off among bandwidth, gain, and profile. The hybrid metasurface antenna (HMA) and dielectric patch resonator (DPR) antennas reported in [19] and [20] exhibit bandwidths of 18.1% and 20.3%, respectively, along with higher gain than the proposed design. However, these advantages come at the expense of increased profile due to their double-layer configurations and additional dielectric resonators. In [21], an MPA employing a composite right/left-handed transmission line structure demonstrates pattern diversity, switching between broadside and conical modes depending on the excited resonant. Although it achieves a higher gain of 10.4 dBi, its narrower fractional bandwidth of 16.5% and multilayer configuration reduces its compactness. Meanwhile, the wideband dielectric resonator antenna (DRA) was reported in [22] achieves a 26% bandwidth by exciting dual modes through a differentially fed substrate integrated cavity. Nevertheless, this performance is accompanied by a relatively high-profile of $0.19\lambda_0$, which is considerably thicker than that of the proposed configuration.

In summary, Table I shows that the proposed antenna offers a balanced combination of bandwidth, gain, and structural compactness. The 18.5% fractional bandwidth fully covers the 5 GHz operating band, ensuring reliable performance for wideband wireless systems. Its low-profile configuration provides a clear advantage for space-limited applications where antenna height becomes a critical design factor. Despite its compact size, the antenna maintains good radiation characteristics, achieving a broadside gain of 4.8 dBi, which is suitable for applications that require stable and directional radiation. These features demonstrate the practical effectiveness of the proposed design for wideband communication scenarios.

IV. Conclusion

A wideband multi-resonant MPA has been designed and characterized through simulation and measurement to demonstrate its performance. The results conclude that the proposed MPA, which employs a slot-loaded U-shaped patch, a parasitic element, and a rectangular ring surrounding the main radiator, can induce multiple adjacent resonant modes, providing a wide bandwidth that covers the entire 5 GHz frequency band. The antenna exhibits a directional radiation pattern with a gain of 4.85 dBi, making it suitable for wireless communication systems, including WLAN and other wideband applications within the operating frequency. Additionally, this multi-resonant MPA maintains a low-profile structure with a simple design and configuration. Further improvements in gain performance will be addressed in future work.

References

[1] International Telecommunication Union. (ITU-R), "Future technology trends of terrestrial International Mobile Telecommunications systems towards 2030 and beyond," Geneva, Switzerland, M.2516-0, 2022.

[2] IEEE Standard Association. "The evolution of Wi-Fi technology and standards." [Online]. Available https://standards.ieee.org/beyond-standards/the-evolution-of-wi-fi-technology-and-standards/.

[3] Z. Xu, Y. Hao, A. Luo, and Y. Jiang, "Technologies and applications in wireless biosensors for real-time health monitoring," *Med-X,* vol. 2, no. 1, 2024, doi: 10.1007/s44258-024-00041-3.

[4] R. K. Crane, *Propagation Handbook for Wireless Communication System Design*. Boca Raton, FL, USA: CRC Press, 2003.

[5] S. R. Saunders and A. Aragon - Zavala, *Antennas and Propagation for Wireless Communication Systems 3e*. Chichester, U.K: Wiley, 2024.

[6] K. Zhang, P. J. Soh, T. Wu, M. Wang, and S. Yan, "A Compact Multimode Antenna Design Based on Metasurface for Wideband Applications," *IEEE Transactions on Antennas and Propagation,* vol. 72, no. 8, pp. 6747-6752, 2024, doi: 10.1109/tap.2024.3408472.

[7] J.-X. Chen, J. Zhou, J. Cai, and W.-W. Yang, "Bandwidth-Enhanced Frequency-Agile Stacked Patch Antenna Sharing Common Tuning Element," *IEEE Antennas and Wireless Propagation Letters,* vol. 23, no. 12, pp. 4313-4317, 2024, doi: 10.1109/lawp.2024.3444793.

[8] C. A. Balanis, *Antenna Theory: Analysis and Design*, 4 ed. Hoboken, New Jersey: Wiley, 2016.

[9] R. Garg, P. Bhartia, I. Bahl, and A. Ittipiboon, *Microstrip Antenna Design Handbook*. Boston, MA, USA: Artech House, 2001.

[10] M. H. Moradi Ardekani and S. Pashangeh, "A novel wideband slot loaded microstrip patch antenna through reallocation of TM1,0, modified TM0,2 and TM1,2 modes," *IET Microwaves, Antennas & Propagation,* vol. 18, no. 11, pp. 860-868, 2024, doi: https://doi.org/10.1049/mia2.12509.

[11] A. K. Awasthi, C. D. Simpson, S. Kolpuke, T. D. Luong, J.-B. Yan, D. Taylor, and S. P. Gogineni, "Ultra-Wideband Patch Antenna Array With an Inclined Proximity Coupled Feed for Small Unmanned Aircraft RADAR Applications," *IEEE Open Journal of Antennas and Propagation,* vol. 2, pp. 1079-1086, 2021, doi: 10.1109/ojap.2021.3128015.

[12] M. M. Rahman *et al.*, "A wideband array antenna with a novel matching circuit and DGS structure for the sub 6 GHz applications," *Scientific Reports,* vol. 15, no. 1, 2025, doi: 10.1038/s41598-025-99517-4.

[13] S.-Y. Tang, J. Chen, N.-W. Liu, G. Fu, L. Zhu, and J. Chen, "A Low-Profile Microstrip Patch Antenna With Enhanced Bandwidth and Pattern Diversity Using Even- and Odd-Order Modes," *IEEE Antennas and Wireless Propagation Letters,* vol. 20, no. 6, pp. 998-1002, 2021, doi: 10.1109/lawp.2021.3069252.

[14] K. T. Lo, W. Sun, and H. Wong, "Design of a Wideband Dielectric Fed Patch Antenna With Multiple Resonances," *IEEE Transactions on Antennas and Propagation,* vol. 73, no. 10, pp. 8301-8306, 2025, doi: 10.1109/tap.2025.3583412.

[15] X. Liu, W. Hu, S. Gao, L. Wen, Q. Luo, R. Xu, and Y. Liu, "A Wideband Triple-Mode Differentially Fed Microstrip Patch Antenna," *IEEE Antennas and Wireless Propagation Letters,* vol. 20, no. 7, pp. 1160-1164, 2021, doi: 10.1109/lawp.2021.3074302.

[16] E. Zhou, Y. Cheng, F. Chen, H. Luo, and X. Li, "Low-Profile High-Gain Wideband Multi-Resonance Microstrip-Fed Slot Antenna with Anisotropic Metasurface," *Progress In Electromagnetics Research,* vol. 175, pp. 91-104, 2022, doi: 10.2528/pier22062201.

[17] A. Bhattacharyya, J. Pal, K. Patra, and B. Gupta, "Bandwidth-Enhanced Miniaturized Patch Antenna Operating at Higher Order Dual-Mode Resonance Using Modal Analysis," *IEEE Antennas and Wireless Propagation Letters,* vol. 20, no. 2, pp. 274-278, 2021, doi: 10.1109/lawp.2020.3048444.

[18] F.-X. Liu, J. Cui, J. Wang, and L. Zhao, "Textile Bandwidth-Enhanced Half-Mode Substrate-Integrated Cavity Antenna With V-Slot for WLAN Communications," *IEEE Antennas and Wireless Propagation Letters,* vol. 22, no. 2, pp. 333-336, 2023, doi: 10.1109/lawp.2022.3210883.

[19] N.-S. Nie, X.-S. Yang, Z. N. Chen, and B.-Z. Wang, "A Low-Profile Wideband Hybrid Metasurface Antenna Array for 5G and WiFi Systems," *IEEE Transactions on Antennas and Propagation,* vol. 68, no. 2, pp. 665-671, 2020, doi: 10.1109/tap.2019.2940367.

[20] S.-C. Tang, X.-Y. Wang, W.-W. Yang, and J.-X. Chen, "Wideband Low-Profile Dielectric Patch Antenna and Array With Anisotropic Property," *IEEE Transactions on Antennas and Propagation,* vol. 68, no. 5, pp. 4091-4096, 2020, doi: 10.1109/tap.2019.2944534.

[21] S. Yan, Y. Zheng, B. Wang, J. Zhang, and G. A. E. Vandenbosch, "A Low-Profile Wideband Microstrip Antenna With Pattern Diversity Based on Composite Right/Left-Handed Transmission Lines," *IEEE Antennas and Wireless Propagation Letters,* vol. 20, no. 8, pp. 1478-1482, 2021, doi: 10.1109/lawp.2021.3087783.

[22] R. Shamsaee Malfajani, J.-J. Laurin, and M. S. Sharawi, "Wideband Substrate Integrated Cavity-Backed Dielectric Resonator Antenna at Sub-6-GHz Band," *IEEE Open Journal of Antennas and Propagation,* vol. 4, pp. 60-68, 2023, doi: 10.1109/ojap.2022.3231892.